Cell Reports

Report

KAT-Independent Gene Regulation by Tip60 Promotes ESC Self-Renewal but Not Pluripotency

Graphical Abstract

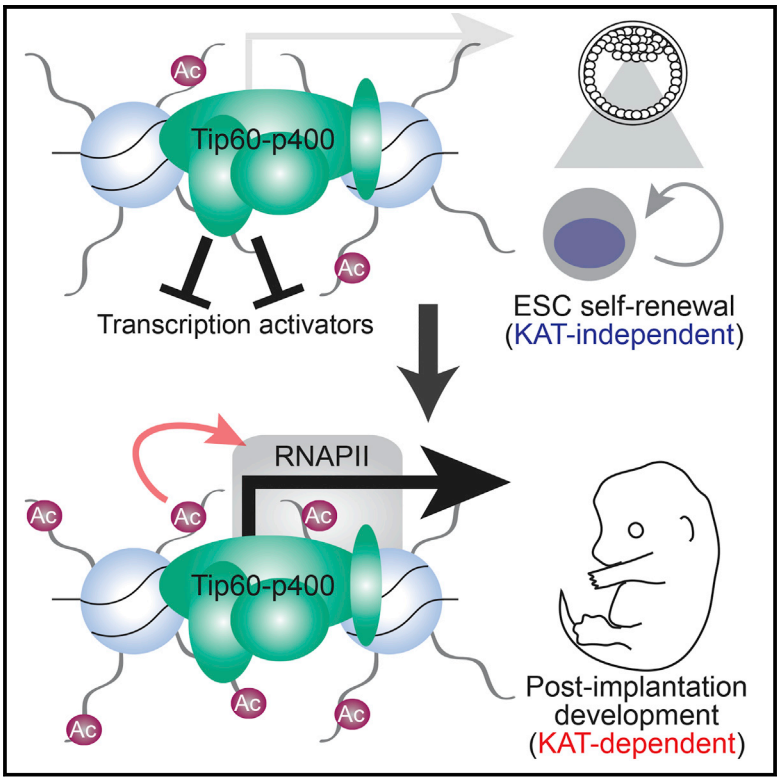

Authors

Diwash Acharya, Sarah J. Hainer, Yeonsoo Yoon, Feng Wang, Ingolf Bach, Jaime A. Rivera-Pérez, Thomas G. Fazzio

Correspondence

thomas.fazzio@umassmed.edu

In Brief

Acharya et al. show that the Tip60 (Kat5) lysine acetyltransferase regulates gene expression and self-renewal independently of its KAT activity in mouse ES cells. The KAT activity is necessary for differentiation and post-implantation mouse development. Therefore, Tip60 has KAT-independent (early) and KAT-dependent (later) functions that are essential for development.

Highlights

- The Tip60 acetylase (KAT) activity is dispensable for gene regulation in ESCs
- Tip60-p400 complex limits chromatin accessibility independently of its KAT activity
- The Tip60 KAT activity is necessary for induction of differentiation genes
- Tip60 KAT mutant mice exhibit developmental defects later than null mutants

Accession Numbers

GSE85505

Acharya et al., 2017, Cell Reports *19*, 671–679
April 25, 2017
http://dx.doi.org/10.1016/j.celrep.2017.04.001

CellPress

Cell Reports
Report

KAT-Independent Gene Regulation by Tip60 Promotes ESC Self-Renewal but Not Pluripotency

Diwash Acharya,[1] Sarah J. Hainer,[1] Yeonsoo Yoon,[2] Feng Wang,[1] Ingolf Bach,[1] Jaime A. Rivera-Pérez,[2] and Thomas G. Fazzio[1,3,*]
[1]Department of Molecular, Cell, and Cancer Biology, University of Massachusetts Medical School, Worcester, MA 01605, USA
[2]Division of Genes and Development, Department of Pediatrics, University of Massachusetts Medical School, Worcester, MA 01605, USA
[3]Lead Contact
*Correspondence: thomas.fazzio@umassmed.edu
http://dx.doi.org/10.1016/j.celrep.2017.04.001

SUMMARY

Although histone-modifying enzymes are generally assumed to function in a manner dependent on their enzymatic activities, this assumption remains untested for many factors. Here, we show that the Tip60 (Kat5) lysine acetyltransferase (KAT), which is essential for embryonic stem cell (ESC) self-renewal and pre-implantation development, performs these functions independently of its KAT activity. Unlike ESCs depleted of *Tip60*, KAT-deficient ESCs exhibited minimal alterations in gene expression, chromatin accessibility at Tip60 binding sites, and self-renewal, thus demonstrating a critical KAT-independent role of Tip60 in ESC maintenance. In contrast, KAT-deficient ESCs exhibited impaired differentiation into mesoderm and endoderm, demonstrating a KAT-dependent function in differentiation. Consistent with this phenotype, KAT-deficient mouse embryos exhibited post-implantation developmental defects. These findings establish separable KAT-dependent and KAT-independent functions of Tip60 in ESCs and during differentiation, revealing a complex repertoire of regulatory functions for this essential chromatin remodeling complex.

INTRODUCTION

Embryonic stem cells (ESCs)—cells derived from the inner cell mass of the early blastocyst—have been utilized as an in vitro model of differentiation due to their pluripotency and unlimited capacity for self-renewal in culture (Keller, 2005). A complex array of signaling pathways and transcription factors control ESC fate, promoting self-renewal in the presence of either leukemia inhibitory factor (LIF) or inhibitors of differentiation-promoting kinases MEK1/2 and Gsk3β (Ying et al., 2008). In addition to transcription factors, a number of chromatin regulatory proteins help control the expression of pro-self-renewal and pro-differentiation genes (Chen and Dent, 2014). Although dozens of chromatin regulators necessary for ESC self-renewal or differentiation have been identified, the specific contributions of many chromatin regulatory proteins to ESC self-renewal and differentiation are poorly understood, due to the redundant and context-dependent contributions of most chromatin modifications to gene expression (Rando and Chang, 2009).

Previously, we showed that RNAi-mediated knockdown (KD) of components of the well-conserved Tip60-p400 (also called NuA4) chromatin regulatory complex resulted in multiple defects in ESC pluripotency (Fazzio et al., 2008a). ESCs depleted of Tip60-p400 subunits exhibit cell and colony morphologies indicative of differentiation and reduced expression of some pluripotency markers. However, Tip60-p400-depleted cells are also defective in normal ESC differentiation, forming small, abnormal embryoid bodies under differentiation conditions that fail to upregulate some markers of differentiated cells (Chen et al., 2013; Fazzio et al., 2008a). Consistent with this self-renewal defect, homozygous knockout of the *Tip60* gene in mouse results in embryonic lethality at approximately the blastocyst stage (the stage at which ESCs are derived) (Hu et al., 2009). $Tip60^{-/-}$ blastocysts are morphologically abnormal and fail to hatch from the zona pellucida when cultured in vitro. No post-implantation $Tip60^{-/-}$ embryos were observed, demonstrating an absolute requirement for *Tip60* at or before this stage.

Tip60-p400 has two biochemical activities that contribute to its functions within the nucleus. The Tip60 subunit is a lysine acetyltransferase (KAT) that targets histones H4 and H2A, H2A variants, and non-histone proteins (Ikura et al., 2000; Keogh et al., 2006; Squatrito et al., 2006; Xu and Price, 2011). Histone acetylation near gene promoters or enhancers is strongly associated with gene expression, consistent with Tip60's known function as a co-activator that collaborates with numerous transcription factors (Squatrito et al., 2006). In addition to its role as a co-activator, Tip60 also directly regulates the activities of numerous transcription factors through acetylation of lysine residues (Farria et al., 2015). Finally, besides regulation of transcription, Tip60 plays important roles in DNA damage repair, senescence, and apoptosis (Doyon et al., 2004; Ikura et al., 2000; Kusch et al., 2004; Xu and Price, 2011; Jiang et al., 2011; Sykes et al., 2006; Tang et al., 2006; Van Den Broeck et al., 2012). Importantly, the KAT activity of Tip60 has been shown to be essential for its role in each of these processes.

The second chromatin remodeling activity found within the Tip60-p400 complex is catalyzed by the p400 subunit (gene name: *Ep400*). The p400 protein, like its homologs in other eukaryotes, catalyzes ATP-dependent incorporation of histone H2A variant H2A.Z into chromatin via exchange of H2A-H2B dimers within nucleosomes for free H2A.Z-H2B dimers (Gévry et al., 2007; Mizuguchi et al., 2004). Interestingly, p400 was recently shown to incorporate histone H3 variant H3.3 into chromatin (Pradhan et al., 2016). H2A.Z and H3.3 are often enriched near gene regulatory regions, consistent with a role for p400 (like Tip60) as a co-activator of transcription (Melters et al., 2015). However, p400 also appears to repress transcription in some contexts as well as promote DNA repair in concert with Tip60 (Gévry et al., 2007; Papamichos-Chronakis et al., 2011; Xu et al., 2012).

How does Tip60-p400 promote ESC self-renewal and pre-implantation development? Tip60-p400 binds near the promoters of both active genes and lowly expressed developmental genes in ESCs and acetylates the promoter-proximal histones of both groups (Chen et al., 2013, 2015; Fazzio et al., 2008a; Ravens et al., 2015). Given the well-established activating roles of histone acetylation, these data imply that Tip60-p400 may drive expression of highly expressed housekeeping and pluripotency genes but that its developmental targets are resistant to this activation, possibly due to the repressive activities of Polycomb complexes or other factors (Aloia et al., 2013; Simon and Kingston, 2013). However, this model is unlikely to be correct, since Tip60-p400 is largely dispensable for transcriptional activation in ESCs, and instead functions mainly to repress its developmental targets (Chen et al., 2013; Fazzio et al., 2008a, 2008b). Therefore, either the Tip60 KAT activity must inhibit transcription of developmental genes in ESCs, or repression of these genes by Tip60-p400 is KAT independent.

Here, we show that Tip60 functions independently of its KAT activity to repress differentiation genes in ESCs and promote ESC self-renewal. Consistent with this repressive function, Tip60 limits promoter-proximal chromatin accessibility at many Tip60 target genes, and this function is similarly KAT independent. By contrast, KAT-deficient ESCs are impaired for differentiation, revealing a critical role for the Tip60 KAT activity in pluripotency. Upon induction of differentiation, KAT mutant ESCs exhibit defects in production of mesoderm and endoderm cell types, due to reduced induction of numerous key drivers of differentiation. Unlike *Tip60* null mice (Hu et al., 2009), KAT-deficient mutant mice proceed past the blastocyst stage, consistent with the ability of KAT mutant ESCs to self-renew. However, KAT mutant mice exhibit post-implantation developmental defects beginning around the start of gastrulation, analogous to the ESC differentiation defect observed in vitro. Together, these findings establish separable KAT-independent and KAT-dependent roles of Tip60 in pluripotency and embryonic development that are both essential but that act at different stages.

RESULTS

Tip60 KAT Activity Is Dispensable for Gene Regulation and Self-Renewal in ESCs

Tip60 is one of several histone acetyltransferases (HATs) that acetylate the N-terminal tails of histones H4 and H2A, whereas p400 is one of two SWI/SNF (switch/sucrose non-fermentable) family ATPases that mediate H2A.Z deposition (Altaf et al., 2009; Lalonde et al., 2014). To test the importance of these activities in ESCs, we generated independent ESC lines with homozygous mutations encoding amino acid substitutions in the acetyl coenzyme A (CoA)-binding site of Tip60 ($Tip60^{ci/ci}$) or the ATP-binding pocket of p400 ($Ep400^{ci/ci}$; Figures S1A and S1B), both of which were previously shown to block enzymatic activity (Ikura et al., 2000; Xu et al., 2010). We confirmed that these mutations broadly reduced H4 acetylation and H2A.Z deposition, respectively, in ESCs (Figures S1C and S1D). Since *Tip60* or *Ep400* depletion in ESCs causes loss of self-renewal (Fazzio et al., 2008a), we utilized previously validated short hairpin RNAs (shRNAs) (Chen et al., 2013) to perform acute KD of *Tip60* or *Ep400*, along with an *Ep400* hypomorphic mutant ($Ep400^{hypo}$) that exhibits reduced levels of p400 protein (Figure S1E), for comparison. Surprisingly, $Tip60^{ci/ci}$ and $Ep400^{ci/ci}$ lines had normal ESC morphology and maintained expression of pluripotency markers such as alkaline phosphatase (AP; Figure 1A), and stage-specific embryonic antigen 1 (SSEA-1) (Figure S1F), whereas *Tip60* KD or $Ep400^{hypo}$ cells exhibited reduced AP and SSEA-1 staining and flattened colony morphologies, as observed previously (Chen et al., 2015; Fazzio et al., 2008a). $Tip60^{ci/ci}$ and $Ep400^{ci/ci}$ cells proliferated more rapidly than *Tip60* KD and $Ep400^{hypo}$ cells (Figure 1B), although $Tip60^{ci/ci}$ cells proliferated slightly less rapidly than wild-type controls. Finally, to test for functional redundancy, we constructed double-homozygous mutant $Tip60^{ci/ci}$ $Ep400^{ci/ci}$ lines. As with the single mutants, these lines expressed markers of pluripotent stem cells and normal ESC colony morphology, similar to that of $Tip60^{ci/ci}$ single mutants (Figures S1F and S1G). These data suggest that loss of Tip60 KAT activity and p400 ATP-dependent nucleosome remodeling activity have minimal effects on ESC maintenance.

To test whether gene expression is altered in $Tip60^{ci/ci}$ and $Ep400^{ci/ci}$ mutant ESCs, in spite of their normal self-renewal, we performed RNA sequencing (RNA-seq) on biological replicates of $Tip60^{ci/ci}$ and $Ep400^{ci/ci}$ mutants, along with positive and negative controls. Consistent with previous findings (Chen et al., 2013; Fazzio et al., 2008a), *Tip60* KD and $Ep400^{hypo}$ cells each exhibited upregulation of numerous genes enriched for developmental factors and downregulation of a smaller group of genes (Figures 1C–1F; Figures S2A and S2B). In contrast, few genes were significantly altered in $Tip60^{ci/ci}$, $Ep400^{ci/ci}$, or $Tip60^{ci/ci}$ $Ep400^{ci/ci}$ double mutants (Figures 1C–1F; Figures S2C–S2F). These data demonstrate that, while Tip60 and p400 are necessary for gene regulation and self-renewal in ESCs, their catalytic activities are dispensable for these processes.

KAT-Independent Regulation of Promoter-Proximal Chromatin Accessibility by Tip60

Since KATs function mainly as co-activators of gene expression, we next focused on how Tip60 functions independently of its KAT activity to repress transcription in ESCs. We confirmed normal expression of Tip60 and p400 in $Tip60^{ci/ci}$ $Ep400^{ci/ci}$ ESCs (Figure S3A) and found that $Tip60^{ci/ci}$ and $Ep400^{ci/ci}$ ESCs assemble intact Tip60-p400 complexes with compositions

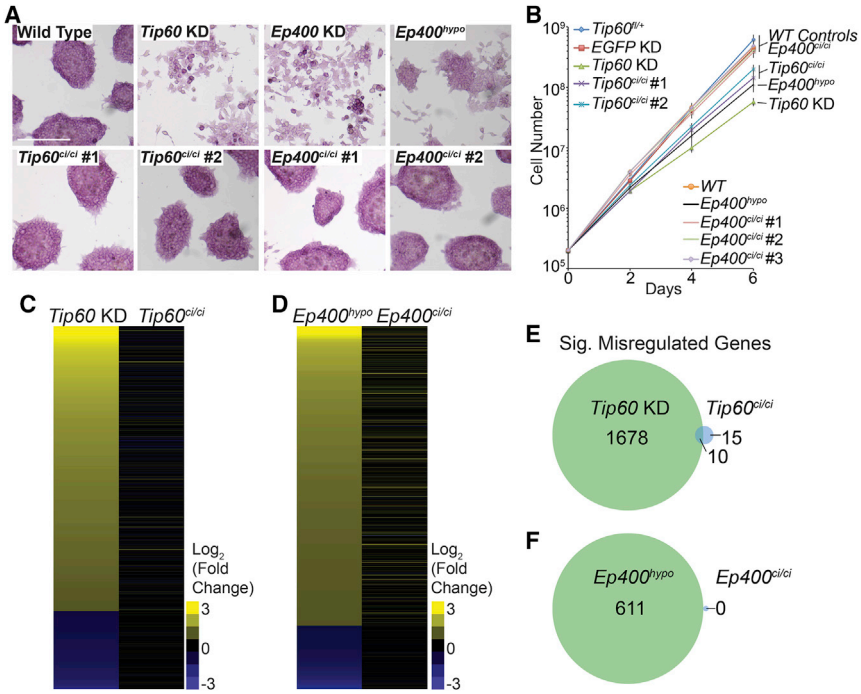

Figure 1. Tip60 KAT and p400 ATPase Activities Are Dispensable for ESC Self-Renewal and Gene Regulation

(A) Alkaline phosphatase (AP) staining of *Tip60*$^{ci/ci}$ and *Ep400*$^{ci/ci}$ mutants and controls (*Tip60*$^{fl/+}$, *Tip60* KD, *Ep400* KD, and *Ep400*^{hypo}). Scale bar, 200 μm.

(B) Growth curve measuring the proliferation rates of the indicated mutant and control ESCs. Error bars represent one SD.

(C and D) Heatmaps of differentially expressed genes in *Tip60*$^{ci/ci}$ and *Tip60* KD ESCs relative to *Tip60*$^{fl/+}$ control cells (C), or *Ep400*$^{ci/ci}$ and *Ep400*^{hypo} ESCs relative to wild-type (E14) control ESCs (D). Genes in the heatmaps are sorted from the most upregulated to the most downregulated genes in the *Tip60* KD and *Ep400*^{hypo} controls, respectively.

(E and F) Venn diagrams showing the number of genes commonly misregulated in *Tip60*$^{ci/ci}$ and *Tip60* KD ESCs (E) or *Ep400*$^{ci/ci}$ and *Ep400*^{hypo} ESCs (F). Genes were considered significantly (Sig.) misregulated in each KD or mutant if their $|\log_2$ (fold change)$| > 1$ and their multiple-testing-adjusted p value < 0.05.

similar to that of wild-type cells, in contrast to *p400*^{hypo} mutant ESCs (Figure S3B).

Given its size (~1.5 MDa; 17 core subunits), we considered the possibility that binding of the Tip60-p400 complex reduces the accessibility of underlying chromatin, regardless of its enzymatic functions. To test this possibility, we performed an assay for transposase-accessible chromatin followed by high-throughput sequencing (ATAC-seq) (Buenrostro et al., 2013) to quantify changes in chromatin accessibility at Tip60-binding sites. In *Tip60*$^{fl/+}$ control ESCs (expressing wild-type *Tip60*), chromatin accessibility is higher at Tip60-binding sites than flanking regions (Figures 2A and 2B), consistent with the observed enrichment of Tip60 near gene regulatory elements such as promoters and enhancers (Chen et al., 2013; Fazzio et al., 2008a; Ravens et al., 2015). Interestingly, we observed significantly increased chromatin accessibility upon *Tip60* KD but minimal changes in accessibility in KAT-deficient ESCs (Figures 2A and 2B). Clustering of these data identified two prominent patterns of chromatin accessibility, segregated primarily by whether the Tip60-binding sites were promoter-proximal or -distal (Figure 2C). Examination of promoter-proximal regions of Tip60 target genes revealed that *Tip60* KD increased chromatin accessibility within a several-hundred base-pair window extending from the promoter into the gene body, corresponding to Tip60-p400 binding sites on chromatin (Figure 2D) (Chen et al., 2013, 2015; Ravens et al., 2015). In contrast, KAT-deficient ESCs were minimally affected. Unlike promoter-proximal regions, chromatin accessibility at gene-distal Tip60-binding sites was relatively unaltered by *Tip60* KD or KAT mutation (Figure 2E). Consistent with these findings, KAT-deficient Tip60 bound to Tip60-p400 target genes at levels similar to those of wild-type (Figure S3C). These data demonstrate Tip60 functions independently of its KAT activity to regulate promoter-proximal chromatin accessibility in ESCs.

Tip60 KAT Activity Is Necessary for Differentiation and Post-implantation Development

Consistent with the self-renewal defect of *Tip60* KD ESCs (Fazzio et al., 2008a), *Tip60* homozygous null (*Tip60*$^{-/-}$) mice die at the peri-implantation stage: *Tip60*$^{-/-}$ blastocysts fail to hatch and survive in culture, and no post-implantation *Tip60*$^{-/-}$ embryos can be recovered (Hu et al., 2009). Since *Tip60*$^{ci/ci}$ ESCs self-renew normally, we next tested whether the Tip60 KAT activity is also dispensable for mouse development. To this end, we generated and intercrossed *Tip60*$^{ci/+}$ heterozygous mice to produce *Tip60*$^{ci/ci}$ homozygotes (see Experimental Procedures for details). However, we recovered no *Tip60*$^{ci/ci}$ pups at birth ($\chi^2 = 40.45$, $p < 0.001$), suggesting that Tip60 KAT activity is essential for development (Figure 3A). To elucidate the developmental defect of *Tip60*$^{ci/ci}$ animals, we examined the morphology of embryos at multiple stages. *Tip60*$^{ci/ci}$ embryos were recovered as late as 10.5 days post-fertilization (embryonic day [E]10.5; Figure 3A) but were much smaller than *Tip60*$^{+/+}$ or *Tip60*$^{ci/+}$ littermates (Figure 3B) and exhibited morphological abnormalities as early as E6.5 (Figures S4A–S4C). The contrasting phenotypes between *Tip60*$^{-/-}$ and *Tip60*$^{ci/ci}$ mice reveal an essential KAT-independent role for Tip60 in pre-implantation development, as well as an essential KAT-dependent role in early post-implantation development.

The phenotypes of *Tip60*$^{ci/ci}$ embryos are evident at or just before gastrulation, where the three primary germ layers are established, suggesting that, although *Tip60*$^{ci/ci}$ ESCs self-renew normally, they may not differentiate properly. We tested this

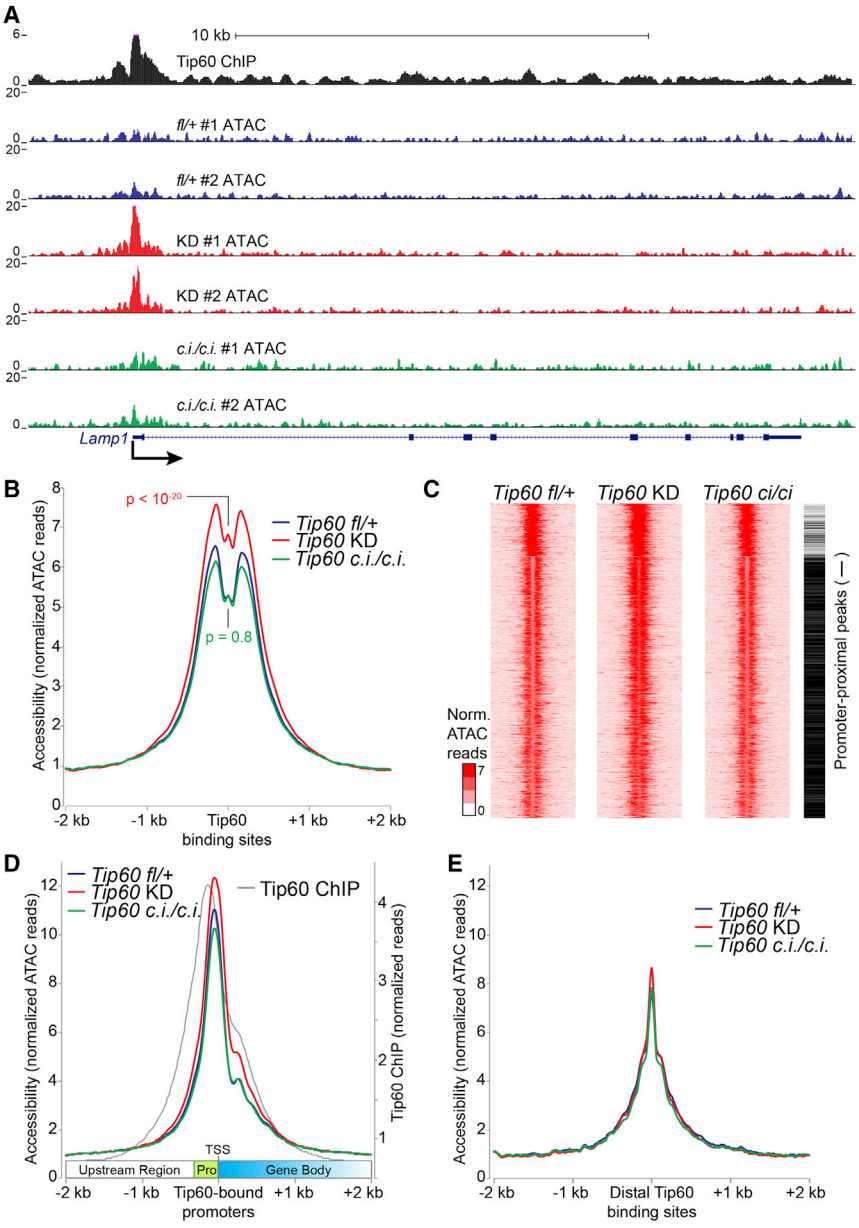

Figure 2. KAT-Independent Regulation of Chromatin Accessibility at Tip60 Target Loci

(A) Example Tip60 target gene showing increased promoter-proximal chromatin accessibility in *Tip60* KD, but not $Tip60^{ci/ci}$, relative to $Tip60^{fl/+}$ control cells. Shown are normalized ATAC-seq reads ≤ 100 bp for each biological replicate and Tip60 ChIP-seq data from Ravens et al. (2015).

(B) Aggregation plot showing average ATAC-seq signal for two biological replicates of each mutant or KD aggregated over high-quality Tip60-binding sites. A Kolmogorov-Smirnov test of differences in ATAC profiles was used to calculate p values.

(C) K-means clustering (K = 3) for ATAC-seq data over Tip60-binding sites. Promoter-proximal peaks are marked with a black bar at the right, and promoter-distal peaks are marked with a white bar. Norm., normalized.

(D) Aggregation plot of ATAC-seq data (as in B) over Tip60-bound promoter regions aligned so that all gene bodies are at the right. Promoter-proximal regions (pro) and transcription start sites (TSS) are indicated. Tip60 ChIP-seq data (Ravens et al., 2015) are shown for reference.

(E) Aggregation plot over Tip60-bound gene-distal regions.

To test whether the ESC differentiation defects were recapitulated in vivo, we stained post-implantation $Tip60^{ci/ci}$ embryos for *T* (also known as *Brachyury*), a marker of cells migrating through the primitive streak to become mesodermal or endodermal cell types (Herrmann, 1991; Rivera-Pérez and Magnuson, 2005). Although *T* staining of $Tip60^{+/+}$ and $Tip60^{ci/+}$ embryos was evident at E6.5 and strong at E7.5, $Tip60^{ci/ci}$ embryos exhibited reduced staining at both stages (Figures 3F and 3G). These data show that gastrulation is delayed or impaired in $Tip60^{ci/ci}$ embryos. This phenotype could result from impaired lineage commitment, poor migration of cells through the primitive streak, or other factors. Regardless, this developmental defect is consistent with the impaired induction of early mesodermal and endodermal markers observed for KAT-defective ESCs in vitro.

possibility using embryoid body differentiations of control, *Tip60* KD, and $Tip60^{ci/ci}$ ESCs. Previously, we showed that KD of *Tip60*, *Ep400*, or (Tip60-p400 subunit) *Dmap1* resulted in defects in embryoid body (EB) formation (Chen et al., 2013; Fazzio et al., 2008a), suggesting that Tip60-p400 is required for this initial step of differentiation. In contrast, $Tip60^{ci/ci}$ ESCs efficiently formed EBs, which expanded in culture at near-wild-type levels, although modest differences in EB morphology were observed relative to $Tip60^{fl/+}$cells (Figures 3C and 3D). However, induction of mesodermal and endodermal markers was delayed and/or reduced in $Tip60^{ci/ci}$ EBs (Figure 3E), compared to $Tip60^{fl/+}$ controls. These data suggest that the Tip60 KAT activity is important for specification of mesodermal and endodermal cell types in vitro.

Impaired Expression of Multiple Drivers of Differentiation in KAT-Deficient ESCs

What is the molecular basis for the in vivo and in vitro developmental defects of $Tip60^{ci/ci}$ mutants? These phenotypes could result from failure to upregulate key lineage-specific transcription factors and/or a disruption in signaling pathways that promote lineage commitment. To address these possibilities, we compared the changes in gene expression during a time course of differentiation of control ($Tip60^{fl/+}$) and $Tip60^{ci/ci}$ ESCs using RNA-seq on biological replicate samples. We

A

	+/+	ci/+	ci/ci	Total	Resorbed	ND
At birth	43	77	0	120	-	-
E10.5	8	16	3	27	3	1
E9.5	8	14	5	27	1	-
E7.5	4	4	2	10	1	-
E6.5	9	22	6	37	10	-

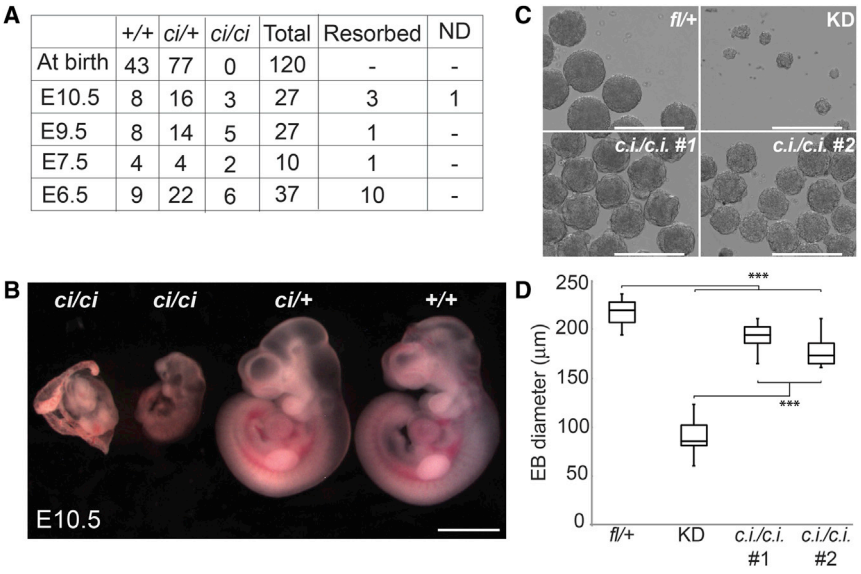

Figure 3. The Tip60 Catalytic Activity Is Required for Differentiation and Post-implantation Development

(A) Genotypes of embryos from *Tip60*$^{ci/+}$ intercrosses at different developmental stages. ND, not determined.

(B) Images of E10.5 embryos of the indicated genotypes. Scale bar, 1 mm.

(C) EB formation assay comparing EB morphology in *Tip60*$^{ci/ci}$ mutant ESCs to *Tip60*$^{fl/+}$ and *Tip60* KD controls. Scale bars, 400 μm.

(D) Quantification of EB size in indicated mutants and controls (n = 49 per genotype). Boxes range from the 25th to the 75th percentile, the middle lines indicate the median, and the whiskers indicate the lesser of either the extreme (maximum or minimum) value or 1.5 times the interquartile range (***$p < 0.001$, calculated using a two-sided t test).

(E) qRT-PCR analysis of indicated germ layer markers during a time course of EB differentiation.

(F and G) Whole-mount in situ hybridization in E6.5 and E7.5 mouse embryos staining for *T* transcript. Scale bars, 100 μm (F) or 250 μm (G).

observed differences in both the timing and levels of markers of mesoderm and endoderm (Figure 4A; e.g., *FoxA2*, *Gata4*, *Sox17*, *T*, *Hand1*, and *Flk1*), expanding on our preliminary analyses (Figure 3E). Next, we used k-means clustering to identify groups of genes induced early or late during differentiation in *Tip60*$^{fl/+}$ control cells and characterized the effects of the KAT mutation on their induction. We observed 1,338 genes of this type that mainly fall into three clusters based on the timing of their expression peak (Figure 4B). In *Tip60*$^{ci/ci}$ cells, we observed reduced or delayed induction of numerous genes with key roles in differentiation, including developmental transcription factors and mediators of growth factor signaling, within each of the three clusters (Figure 4B).

To test whether impaired induction of key signaling proteins hindered activation of their downstream targets, we examined activation of the FGF/MEK/ERK (fibroblast growth factor/mitogen-activated protein kinase kinase/extracellular signal-regulated kinase) and TGF-β (transforming growth factor β) pathways using antibodies recognizing the phosphorylated (and activated) forms of ERK1/2 and Smad2/3, respectively (Tsang and Dawid, 2004; Whitman and Mercola, 2001). These factors act downstream of FGF and BMP (bone morphogenetic protein) signaling in differentiating ESCs and embryos and are critical for differentiation (Sui et al., 2013). Although Smad2/3 phosphorylation was unaltered in differentiating *Tip60*$^{ci/ci}$ ESCs, we observed impaired ERK phosphorylation in these mutants after 6 days of differentiation (Figure 4C). Together, these data suggest that the differentiation defect observed in *Tip60*$^{ci/ci}$ ESCs is due to at least two overlapping defects: delayed or reduced activation of ERK and impaired induction of key developmental transcription factors.

DISCUSSION

Here, we showed that Tip60 functions in ESC gene regulation and self-renewal, as well as pre-implantation development, independently of its KAT activity. This finding was unexpected,

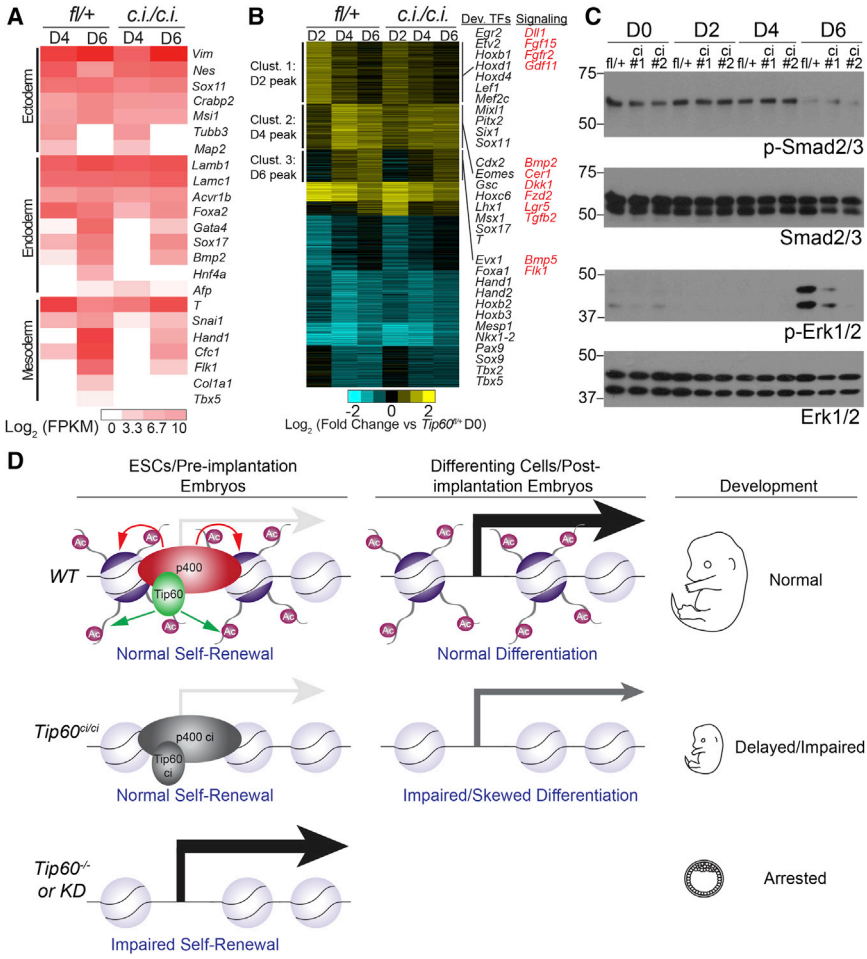

Figure 4. Delayed and Impaired Expression of Developmental Regulators in Differentiating *Tip60*$^{ci/ci}$ ESCs

(A) Heatmap indicating induction kinetics of each germ layer markers during differentiation of *Tip60*$^{fl/+}$ controls or *Tip60*$^{ci/ci}$ mutant ESCs. FPKM, fragments Per kilobase of transcript per million mapped reads.

(B) K-means clustering (K = 9) of differentially expressed genes ($|\log_2$ (fold change)$| > 0.7$; multiple-testing-adjusted p value < 0.05) in *Tip60*$^{fl/+}$ controls or *Tip60*$^{ci/ci}$ mutant ESCs during the differentiation time course. Large upregulated clusters are noted. Key regulatory proteins with impaired induction in *Tip60*$^{ci/ci}$ mutant ESCs are highlighted.

(C) Western blots (one of two independent experiments with similar results) of phosphorylated and total Smad2/3 and Erk1/2 during differentiation in *Tip60*$^{fl/+}$ or *Tip60*$^{ci/ci}$ ESCs.

(D) Model indicating the KAT-independent role of Tip60 in ESC self-renewal and gene regulation, as well as pre-implantation development, and the KAT-dependent role of Tip60 in differentiation and post-implantation development. See Discussion for additional details. WT, wild-type.

because Tip60 depletion or knockout leads to a self-renewal defect in ESCs and pre-implantation lethality in mice (Fazzio et al., 2008a; Hu et al., 2009). Furthermore, KAT-impaired mutants of *esa1*, the yeast homolog of *Tip60*, are severely growth impaired (Selleck et al., 2005), suggesting that the critical cellular functions of this KAT are dependent on its acetylation activity.

The fact that Tip60 is largely a repressor of transcription in ESCs (Fazzio et al., 2008a), and that this repressive function is independent of its KAT activity, suggests that Tip60 regulates ESC gene expression in a manner that is distinct from other well-studied KATs, at least in part. Consistent with its role as a broadly acting repressor of transcription in ESCs, we found that Tip60 functions by a KAT-independent mechanism to limit chromatin accessibility directly over its promoter-proximal binding sites at many target genes. Additional studies will be necessary to determine whether Tip60 also performs this function in somatic cell types.

In contrast, the Tip60 KAT activity is essential during ESC differentiation and post-implantation development. Consequently, these findings demonstrate separable, essential functions of Tip60: its KAT-independent function is sufficient for Tip60's essential role in ESC self-renewal and pre-implantation development, and its KAT-dependent function is required for post-implantation development and ESC differentiation. Interestingly, we found that the ATP-dependent histone exchange activity of p400 was also dispensable for gene regulation and self-renewal in ESCs, revealing that the Tip60-p400 complex represses differentiation genes in ESCs independently of its known chromatin-remodeling activities (Figure 4D). These findings necessitate a re-evaluation of current models of gene regulation by this essential chromatin regulatory complex.

What is the role of the Tip60 KAT activity during development? Given the defect of KAT-deficient ESCs and embryos in lineage specification, one possibility is that histone acetylation at differentiation genes in ESCs (as observed previously; Fazzio et al., 2008a) facilitates their upregulation when differentiation is induced. This provides a potential explanation for the counterintuitive role of Tip60 in the repression of differentiation genes in ESCs: occupancy of Tip60-p400 at differentiation gene promoters helps repress these genes by reducing chromatin accessibility, while acetylation at these loci may allow more rapid induction after binding of differentiation-specific transcription factors. Together, these data show that not all functions of Tip60 are reliant on its KAT activity, and they raise the possibility that KAT-independent gene regulation by Tip60 plays important roles in additional cell types.

EXPERIMENTAL PROCEDURES

Antibodies

Antibodies used in this study were as follows: p400 (A300-541A; Bethyl Laboratories); StainAlive SSEA-1 (09-0067; Stemgent); Smad2/3 (8685; Cell

Signaling Technologies); Phospho-Smad2/3 (8828; Cell Signaling Technologies); Erk1/2 (9102; Cell Signaling Technologies); Phospho-Erk1/2 (9101; Cell Signaling Technologies); H2AZ (ab4174; Abcam); Acetyl-H4 (06-598; Millipore); FLAG-M2 (F1804; Sigma); IgG ([immunoglobulin G] ab37415; Abcam); and β-actin (A5316; Sigma).

Cell Lines

Mouse ESC lines were derived from E14 (129/Ola) (Hooper et al., 1987) and grown as described previously (Chen et al., 2013). *Tip60*$^{ci/ci}$ ESCs were derived from floxed Tip60-H3F cells (Chen et al., 2013) by introduction of Cre recombinase (Addgene, 20781) to loop out a fused version of wild-type *Tip60* exons 11–14, leaving a mutant exon 11 that harbors two substitution mutations (Q377E and G380E) that eliminate acetyl-CoA binding (Ikura et al., 2000) (Figure S1A).

Catalytically inactive mutants of p400 (*Ep400*$^{ci/ci}$) were generated using homologous recombination stimulated by CRISPR (clustered regularly interspaced short palindromic repeats)/Cas9-mediated cleavage (Cong et al., 2013; Mali et al., 2013). A repair template (Table S3) was synthesized (Integrated DNA Technologies), cloned into pCR2.1, and introduced together with the CRISPR /Cas9 vector (a variant of plasmid pX330 that expresses puromycin resistance). The *Ep400*^{hypo} mutant line, described previously (Chen et al., 2015), was generated using the same CRISPR/Cas9 construct, but without the repair template, resulting in a homozygous 135-bp in-frame deletion that disrupts the ATPase domain and results in lower expression of p400 protein (Figure S1E).

ESC Differentiation

EBs for growth/morphology assays were formed using hanging drops containing 100 cells in 10 μl of differentiation medium. Morphology was examined after 48 hr. For gene expression assays, 10^6 ESCs were plated on non-adherent plates for 48 hr to form EBs and then transferred into gelatinized six-well plates at a low density. Cells were harvested using TRIzol reagent (Invitrogen) at indicated time points. RNA was prepared, and qRT-PCR was performed as described previously (Chen et al., 2013), using primers listed in Table S1.

Cell Staining

10^5 ESCs were grown on gelatin-coated six-well plates for 48 hr. AP staining was performed using a kit (EMD Millipore, SCR004), following the manufacturers' guidelines. SSEA-1 staining of live ESCs was also performed per the manufacturers' instructions (Stemgent, 09-0067).

Tip60-p400 Purification

Tip60-p400 complex was purified from nuclear extracts of wild-type, Tip60$^{ci/ci}$, p400$^{ci/ci}$, and p400^{hypo} cells with endogenous 6×his/3×FLAG tags at the *Tip60* locus, as described previously (Chen et al., 2013). Purified proteins were separated on SDS-PAGE gels, and silver staining was performed using a Silver Staining Kit (ThermoFisher, LC6100).

Western Blotting

30 μg of nuclear extract per lane (prepared using the NE-PER Kit; ThermoFisher, 78833) were used for western blotting.

Generation of *Tip60*$^{ci/ci}$ Mice

Tip60$^{ci/+}$ heterozygous mice were generated by crossing *Tip60* floxed mice (Chen et al., 2013) with the allele described earlier with Tg(EIIa-cre) mice, which broadly express Cre recombinase (Dooley et al., 1989; Lakso et al., 1996). Mice were genotyped by PCR with primers listed in Table S2. *Tip60*$^{ci/+}$ mice were maintained as heterozygotes on an inbred FVB/N background and intercrossed to generate *Tip60*$^{+/+}$, *Tip60*$^{ci/+}$, and *Tip60*$^{ci/ci}$ embryos. Animal studies were performed in accordance with the guidelines of the Institutional Animal Care and Use Committee at the University of Massachusetts Medical School (A-2165) and NIH.

RNA In Situ Hybridization

Whole-mount in situ hybridization was performed as previously described (Rivera-Pérez and Magnuson, 2005), using a full-length cDNA probe of *T* (Herrmann, 1991). Embryos were genotyped after staining by PCR, using primers listed in Table S2.

Chromatin Immunoprecipitation

Chromatin immunoprecipitation and deep sequencing were performed as described previously (Chen et al., 2013; Hainer et al., 2015). Chromatin immunoprecipitation (ChIP)-qPCR was performed using SYBR FAST (KAPA Biosystems), with primers described previously (Fazzio et al., 2008a).

RNA-Seq

Strand-specific library construction and RNA-seq were performed by Applied Biological Materials and the UCLA Clinical Microarray Core for ESCs and differentiating ESCs, respectively. Data analysis is described in the Supplemental Experimental Procedures.

ATAC Sequencing

ATAC sequencing (ATAC-seq) was performed essentially as described previously (Buenrostro et al., 2013, 2015). Two independent ATAC reactions per biological replicate were performed, using 35,000 and 70,000 ESCs each. After library preparation, the two reactions were found to have indistinguishable distributions of fragment sizes and were, therefore, combined for sequencing. (Therefore, each biological replicate consisted of two ATAC reactions.) Data analysis is described in the Supplemental Experimental Procedures.

Statistical Methods

For non-genomic in vitro experiments, two-tailed t tests were used to calculate statistical significance. A chi-square test was used to evaluate genotypes of offspring from Tip60ci/+ intercrosses. Adjusted p values were calculated for RNA-seq data using DEseq2. Significance of differences in ATAC-seq read enrichment were calculated by a hypergeometric test using the *dhyper* package in R.

ACCESSION NUMBERS

The accession number for the deep-sequencing data reported in this paper is GEO: GSE85505.

SUPPLEMENTAL INFORMATION

Supplemental Information includes Supplemental Experimental Procedures, four figures, and three tables and can be found with this article online at http://dx.doi.org/10.1016/j.celrep.2017.04.001.

AUTHOR CONTRIBUTIONS

D.A., J.A.R.-P., and T.G.F. designed experiments. D.A. performed most experiments with help from Y.Y. and J.A.R.-P. (early embryo dissection and staining), F.W. and I.B. (late embryo dissection), and T.G.F. (ATAC-seq). S.J.H. and D.A. analyzed the deep-sequencing data.

ACKNOWLEDGMENTS

We thank J. Benanti and T. Tsukiyama for critical reading of the manuscript. This work was supported by NIH grants R01HD072122 (to T.G.F.), R01HD083311 (to J.A.R.-P.), and R01CA131158 (to I.B.). T.G.F. is supported as a Leukemia and Lymphoma Society Scholar. S.J.H. is a Special Fellow of the Leukemia and Lymphoma Society.

Received: September 23, 2016
Revised: March 1, 2017
Accepted: March 30, 2017
Published: April 25, 2017

REFERENCES

Aloia, L., Di Stefano, B., and Di Croce, L. (2013). Polycomb complexes in stem cells and embryonic development. Development *140*, 2525–2534.

Altaf, M., Auger, A., Covic, M., and Côté, J. (2009). Connection between histone H2A variants and chromatin remodeling complexes. Biochem. Cell Biol. *87*, 35–50.

Buenrostro, J.D., Giresi, P.G., Zaba, L.C., Chang, H.Y., and Greenleaf, W.J. (2013). Transposition of native chromatin for fast and sensitive epigenomic profiling of open chromatin, DNA-binding proteins and nucleosome position. Nat. Methods *10*, 1213–1218.

Buenrostro, J.D., Wu, B., Chang, H.Y., and Greenleaf, W.J. (2015). ATAC-seq: A method for assaying chromatin accessibility genome-wide. Curr. Protoc. Mol. Biol. *109*, 21.29.1–21.29.9.

Chen, T., and Dent, S.Y.R. (2014). Chromatin modifiers and remodellers: regulators of cellular differentiation. Nat. Rev. Genet. *15*, 93–106.

Chen, P.B., Hung, J.-H., Hickman, T.L., Coles, A.H., Carey, J.F., Weng, Z., Chu, F., and Fazzio, T.G. (2013). Hdac6 regulates Tip60-p400 function in stem cells. eLife *2*, e01557.

Chen, P.B., Chen, H.V., Acharya, D., Rando, O.J., and Fazzio, T.G. (2015). R loops regulate promoter-proximal chromatin architecture and cellular differentiation. Nat. Struct. Mol. Biol. *22*, 999–1007.

Cong, L., Ran, F.A., Cox, D., Lin, S., Barretto, R., Habib, N., Hsu, P.D., Wu, X., Jiang, W., Marraffini, L.A., and Zhang, F. (2013). Multiplex genome engineering using CRISPR/Cas systems. Science *339*, 819–823.

Dooley, T.P., Miranda, M., Jones, N.C., and DePamphilis, M.L. (1989). Transactivation of the adenovirus EIIa promoter in the absence of adenovirus E1A protein is restricted to mouse oocytes and preimplantation embryos. Development *107*, 945–956.

Doyon, Y., Selleck, W., Lane, W.S., Tan, S., and Côté, J. (2004). Structural and functional conservation of the NuA4 histone acetyltransferase complex from yeast to humans. Mol. Cell. Biol. *24*, 1884–1896.

Farria, A., Li, W., and Dent, S.Y.R. (2015). KATs in cancer: functions and therapies. Oncogene *34*, 4901–4913.

Fazzio, T.G., Huff, J.T., and Panning, B. (2008a). An RNAi screen of chromatin proteins identifies Tip60-p400 as a regulator of embryonic stem cell identity. Cell *134*, 162–174.

Fazzio, T.G., Huff, J.T., and Panning, B. (2008b). Chromatin regulation Tip(60)s the balance in embryonic stem cell self-renewal. Cell Cycle *7*, 3302–3306.

Gévry, N., Chan, H.-M., Laflamme, L., Livingston, D.M., and Gaudreau, L. (2007). p21 transcription is regulated by differential localization of histone H2A.Z. Genes Dev. *21*, 1869–1881.

Hainer, S.J., Gu, W., Carone, B.R., Landry, B.D., Rando, O.J., Mello, C.C., and Fazzio, T.G. (2015). Suppression of pervasive noncoding transcription in embryonic stem cells by esBAF. Genes Dev. *29*, 362–378.

Herrmann, B.G. (1991). Expression pattern of the Brachyury gene in whole-mount TWis/TWis mutant embryos. Development *113*, 913–917.

Hooper, M., Hardy, K., Handyside, A., Hunter, S., and Monk, M. (1987). HPRT-deficient (Lesch-Nyhan) mouse embryos derived from germline colonization by cultured cells. Nature *326*, 292–295.

Hu, Y., Fisher, J.B., Koprowski, S., McAllister, D., Kim, M.-S., and Lough, J. (2009). Homozygous disruption of the Tip60 gene causes early embryonic lethality. Dev. Dyn. *238*, 2912–2921.

Ikura, T., Ogryzko, V.V., Grigoriev, M., Groisman, R., Wang, J., Horikoshi, M., Scully, R., Qin, J., and Nakatani, Y. (2000). Involvement of the TIP60 histone acetylase complex in DNA repair and apoptosis. Cell *102*, 463–473.

Jiang, Z., Kamath, R., Jin, S., Balasubramani, M., Pandita, T.K., and Rajasekaran, B. (2011). Tip60-mediated acetylation activates transcription independent apoptotic activity of Abl. Mol. Cancer *10*, 88.

Keller, G. (2005). Embryonic stem cell differentiation: emergence of a new era in biology and medicine. Genes Dev. *19*, 1129–1155.

Keogh, M.-C., Mennella, T.A., Sawa, C., Berthelet, S., Krogan, N.J., Wolek, A., Podolny, V., Carpenter, L.R., Greenblatt, J.F., Baetz, K., and Buratowski, S. (2006). The Saccharomyces cerevisiae histone H2A variant Htz1 is acetylated by NuA4. Genes Dev. *20*, 660–665.

Kusch, T., Florens, L., Macdonald, W.H., Swanson, S.K., Glaser, R.L., Yates, J.R., 3rd, Abmayr, S.M., Washburn, M.P., and Workman, J.L. (2004). Acetylation by Tip60 is required for selective histone variant exchange at DNA lesions. Science *306*, 2084–2087.

Lakso, M., Pichel, J.G., Gorman, J.R., Sauer, B., Okamoto, Y., Lee, E., Alt, F.W., and Westphal, H. (1996). Efficient in vivo manipulation of mouse genomic sequences at the zygote stage. Proc. Natl. Acad. Sci. USA *93*, 5860–5865.

Lalonde, M.E., Cheng, X., and Côté, J. (2014). Histone target selection within chromatin: an exemplary case of teamwork. Genes Dev. *28*, 1029–1041.

Mali, P., Yang, L., Esvelt, K.M., Aach, J., Guell, M., DiCarlo, J.E., Norville, J.E., and Church, G.M. (2013). RNA-guided human genome engineering via Cas9. Science *339*, 823–826.

Melters, D.P., Nye, J., Zhao, H., and Dalal, Y. (2015). Chromatin dynamics in vivo: a game of musical chairs. Genes (Basel) *6*, 751–776.

Mizuguchi, G., Shen, X., Landry, J., Wu, W.-H., Sen, S., and Wu, C. (2004). ATP-driven exchange of histone H2AZ variant catalyzed by SWR1 chromatin remodeling complex. Science *303*, 343–348.

Papamichos-Chronakis, M., Watanabe, S., Rando, O.J., and Peterson, C.L. (2011). Global regulation of H2A.Z localization by the INO80 chromatin-remodeling enzyme is essential for genome integrity. Cell *144*, 200–213.

Pradhan, S.K., Su, T., Yen, L., Jacquet, K., Huang, C., Côté, J., Kurdistani, S.K., and Carey, M.F. (2016). EP400 deposits H3.3 into promoters and enhancers during gene activation. Mol. Cell *61*, 27–38.

Rando, O.J., and Chang, H.Y. (2009). Genome-wide views of chromatin structure. Annu. Rev. Biochem. *78*, 245–271.

Ravens, S., Yu, C., Ye, T., Stierle, M., and Tora, L. (2015). Tip60 complex binds to active Pol II promoters and a subset of enhancers and co-regulates the c-Myc network in mouse embryonic stem cells. Epigenetics Chromatin *8*, 45.

Rivera-Pérez, J.A., and Magnuson, T. (2005). Primitive streak formation in mice is preceded by localized activation of Brachyury and Wnt3. Dev. Biol. *288*, 363–371.

Selleck, W., Fortin, I., Sermwittayawong, D., Côté, J., and Tan, S. (2005). The *Saccharomyces cerevisiae* Piccolo NuA4 histone acetyltransferase complex requires the Enhancer of Polycomb A domain and chromodomain to acetylate nucleosomes. Mol. Cell. Biol. *25*, 5535–5542.

Simon, J.A., and Kingston, R.E. (2013). Occupying chromatin: Polycomb mechanisms for getting to genomic targets, stopping transcriptional traffic, and staying put. Mol. Cell *49*, 808–824.

Squatrito, M., Gorrini, C., and Amati, B. (2006). Tip60 in DNA damage response and growth control: many tricks in one HAT. Trends Cell Biol. *16*, 433–442.

Sui, L., Bouwens, L., and Mfopou, J.K. (2013). Signaling pathways during maintenance and definitive endoderm differentiation of embryonic stem cells. Int. J. Dev. Biol. *57*, 1–12.

Sykes, S.M., Mellert, H.S., Holbert, M.A., Li, K., Marmorstein, R., Lane, W.S., and McMahon, S.B. (2006). Acetylation of the p53 DNA-binding domain regulates apoptosis induction. Mol. Cell *24*, 841–851.

Tang, Y., Luo, J., Zhang, W., and Gu, W. (2006). Tip60-dependent acetylation of p53 modulates the decision between cell-cycle arrest and apoptosis. Mol. Cell *24*, 827–839.

Tsang, M., and Dawid, I.B. (2004). Promotion and attenuation of FGF signaling through the Ras-MAPK pathway. Sci. STKE *2004*, pe17.

Van Den Broeck, A., Nissou, D., Brambilla, E., Eymin, B., and Gazzeri, S. (2012). Activation of a Tip60/E2F1/ERCC1 network in human lung adenocarcinoma cells exposed to cisplatin. Carcinogenesis *33*, 320–325.

Whitman, M., and Mercola, M. (2001). TGF-beta superfamily signaling and left-right asymmetry. Sci. STKE *2001*, re1.

Xu, Y., and Price, B.D. (2011). Chromatin dynamics and the repair of DNA double strand breaks. Cell Cycle *10*, 261–267.

Xu, Y., Sun, Y., Jiang, X., Ayrapetov, M.K., Moskwa, P., Yang, S., Weinstock, D.M., and Price, B.D. (2010). The p400 ATPase regulates nucleosome stability and chromatin ubiquitination during DNA repair. J. Cell Biol. *191*, 31–43.

Xu, Y., Ayrapetov, M.K., Xu, C., Gursoy-Yuzugullu, O., Hu, Y., and Price, B.D. (2012). Histone H2A.Z controls a critical chromatin remodeling step required for DNA double-strand break repair. Mol. Cell *48*, 723–733.

Ying, Q.-L., Wray, J., Nichols, J., Batlle-Morera, L., Doble, B., Woodgett, J., Cohen, P., and Smith, A. (2008). The ground state of embryonic stem cell self-renewal. Nature *453*, 519–523.

Cell Reports, Volume *19*

Supplemental Information

KAT-Independent Gene Regulation by Tip60 Promotes ESC Self-Renewal but Not Pluripotency

Diwash Acharya, Sarah J. Hainer, Yeonsoo Yoon, Feng Wang, Ingolf Bach, Jaime A. Rivera-Pérez, and Thomas G. Fazzio

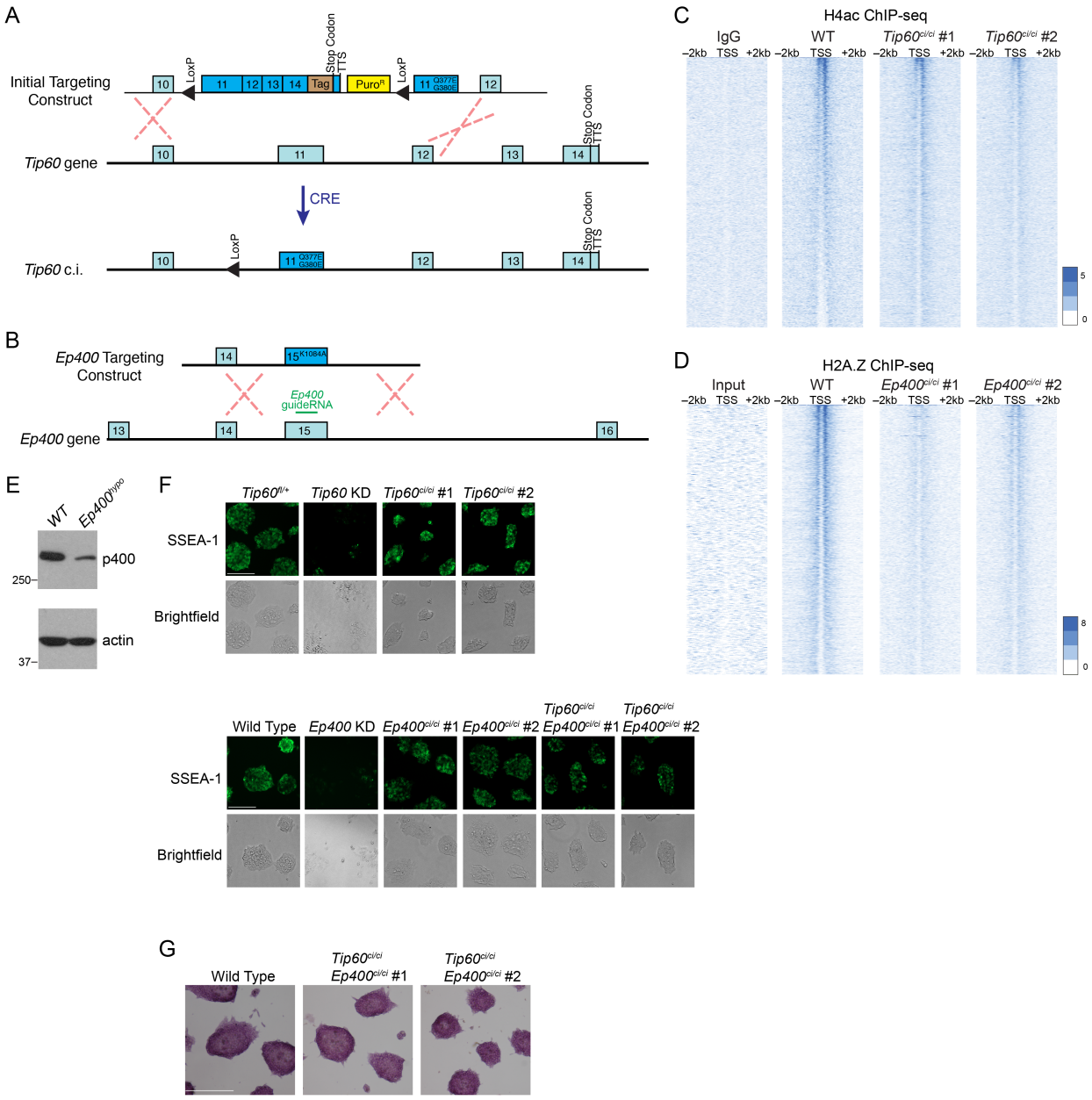

Figure S1. Generation and phenotypes of *Tip60*$^{ci/ci}$ and *Ep400*$^{ci/ci}$ mutants, Related to Figure 1. (**A**) Schematic representation of *Tip60*$^{ci/ci}$ lines generated using homologous recombination of the construct, followed by Cre-LoxP–mediated excision of the wild type *Tip60* sequence. (**B**) Schematic for generation of *Ep400*$^{ci/ci}$ mutants using CRISPR/Cas9 mediated homologous recombination. (**C**) ChIP-seq of tetra-acetylated H4 (K5/8/12/16) in wild type and two *Tip60*$^{ci/ci}$ lines. Heatmaps are over TSS-proximal regions (+/- 2kb), sorted from highest H4ac to lowest. IgG is a specificity control. (**D**) H2A.Z ChIP-seq in wild type or two *Ep400*$^{ci/ci}$ mutant ESC lines, as in (**C**). (**E**) Western blot confirmation of *Ep400*^{hypo} lines, generated using CRISPR/Cas9 without the repair template. (**F**) SSEA-1 live cell staining of *Tip60*$^{ci/ci}$, *Ep400*$^{ci/ci}$, and *Tip60*$^{ci/ci}$*Ep400*$^{ci/ci}$ mutants, compared to their respective controls *Tip60*$^{fl/+}$, *Tip60* KD, Wild Type and *Ep400* KD. (**G**) AP staining of *Tip60*$^{ci/ci}$*Ep400*$^{ci/ci}$ mutants as in Figure 1A. Scale bars equal 200 mm in both (**F**) and (**G**).

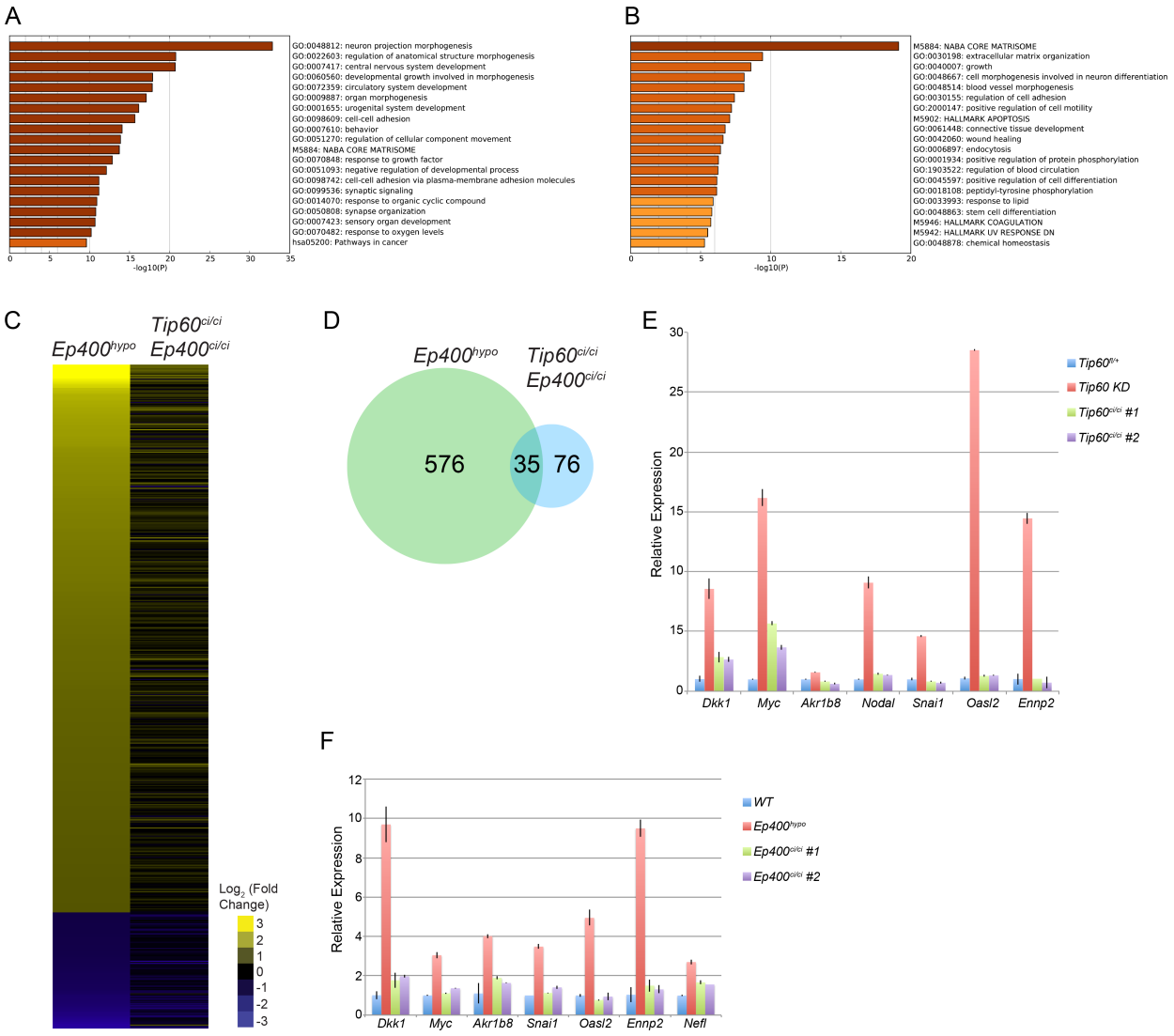

Figure S2. Catalytic activity-independent gene regulation by Tip60-p400, Related to Figure 1. (**A, B**) GO (Gene ontology) terms enriched within genes upregulated in *Tip60* KD (**A**), and *Ep400*^{hypo} ESCs (**B**), as measured by RNAseq. Shown are histograms depicting the significance (-log$_{10}$ p value) of GO categories enriched in each gene set (generated by Metascape; http://metascape.org). (**C**) Heatmaps of differentially expressed genes in *Tip60*$^{ci/ci}$ *Ep400*$^{ci/ci}$ ESCs relative to *Ep400*^{hypo} control cells, as in Figure 1. (**D**) Venn diagram showing number of significantly misregulated genes commonly misregulated in *Tip60*$^{ci/ci}$*Ep400*$^{ci/ci}$ and *Ep400*^{hypo} ESCs, as in Figure 1. (**E, F**) RT-qPCR measuring mRNA levels of Tip60-p400 target genes in mutants or control ESCs as indicated. mRNA levels were normalized to *GAPDH*.

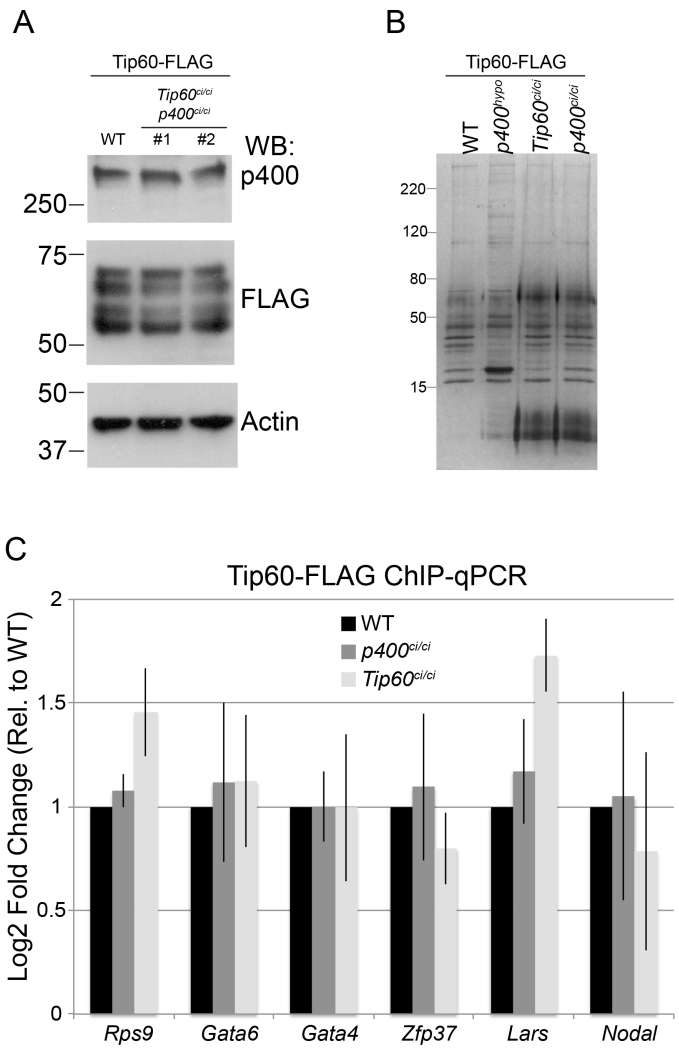

Figure S3. Catalytically inactive Tip60-p400 mutations do not compromise complex integrity, Related to Figure 2. (**A**) Western blots indicating equal expression of catalytic subunits of Tip60-p400 in wild type or double catalytically inactive mutant ESCs. Actin is a loading control. (**B**) Silver stain of Tip60-p400 complex purified from lines with genotypes indicated at top. In each case, Tip60 is FLAG-tagged at both copies of its endogenous locus. (**C**) Tip60-FLAG ChIP-qPCR from WT, *Tip60*$^{ci/ci}$, and *Ep400*$^{ci/ci}$ ESCs show similar Tip60 occupancy in each. Shown are biological triplicate ChIP-qPCRs from each line, normalized to untagged control ESCs, and expressed relative to WT.

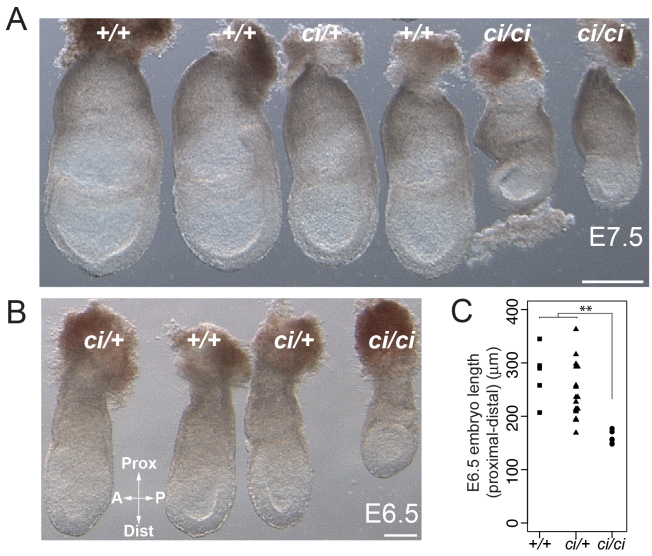

Figure S4. Phenotypes of *Tip60*$^{ci/ci}$ embryos, Related to Figure 3. (**A, B**) Brightfield images of E7.5 and E6.5 embryos from *Tip60*$^{ci/ci}$ intercrosses, with their genotypes (determined after imaging) indicated. Scale bars equal 100 mm. (**C**) Measurement of the length of the proximal distal axis of embryos (epiblast + extraembryonic endoderm) of the indicated genotypes (**p < 0.01, calculated using a two sided t-test).

Table S1. RTqPCR primers, Related to Figure 3.

Nestin	Forward: TGGCACACCTCAAGATGTCCCTTA Reverse: AAGGAAATGCAGCTTCAGCTTGGG
Sox11	Forward: ACGACCTCATGTTCGACCTGAGCT Reverse: CACCAGCGACAGGGACAGGTTC
T	Forward: CCAAGGACAGAGAGACGGCT Reverse: AGTAGGCATGTTCCAAGGGC
Flk1	Forward: GCTTGCTCCTTCCTCATCTC Reverse: CCATCAGGAAGCCACAAAGC
Sox17	Forward: CTCGGGGATGTAAAGGTGAA Reverse: GCTTCTCTGCCAAGGTCAAC
FoxA2	Forward: CCCTACGCCAACATGAACTCG Reverse: GTTCTGCCGGTAGAAAGGGA
Dkk1	Forward: ACTCAAATGGCTTTGGTAATATGG Reverse: ATAATCTCTTCTGAATTCTGCCCA
Myc	Forward: AGCTGTTTGAAGGCTGGATTTC Reverse: GCAACATAGGATGGAGAGCAGA
Akr1b8	Forward: TACTGTCACTCGAAGGGCATCT Reverse: ATCTCCTCGTCACTCAACTGGA
Nodal	Forward: TCCTTCTTCTTCAAGCCTGTTG Reverse: CCAGATCCTCTTCTTGGCTCA
Snai1	Forward: CTTGTGTCTGCACGACCTGTG Reverse: AGACTCTTGGTGCTTGTGGAG
Oasl2	Forward: TTGTGCGGAGGATCAGGTACT Reverse: TGATGGTGTCGCAGTCTTTGA
Ennp2	Forward: ATGGCAAGACAAGGCTGTTTC Reverse: TTGACGCCGATGGCAAAAGT
Scamp1	Forward: CCTTGAGGTCTGTGGTATTGGA Reverse: TACACCCTTAGTGACCTCAGTGTC
Nefl	Forward: AGCTAGAGGACAAGCAGAATGC Reverse: GCAAGCCACTGTAAGCAGAAC

Supplemental Table S2. Genotyping primers, related to Figure 3.

Tip60$^{ci/+}$ or *Tip60*$^{ci/ci}$ (mice and ESCs)	Forward: GTGGGCTACTTCTCCAAGGTC Reverse: TGTGAAGCACAGATGAGGGT

Supplemental Table S3. *Ep400* repair template, related to Figures S1-S3 and Figure 1.

(**K1084A mutation**; silent PAM mutation; *guideRNA sequence*)
TAGGCTCATAAAACTCACAGCAGTCTGAGTTGTGTCTATTTCATTGTTGTTGTAGATGTAGAAGACTG TCCTAGTGACAGGGAGAGCCGGAGGGACTCCGTTCTCATTGACTCACTCTTCATCATGGATCAGTTT AAAGCTGCAGAGAGAATGAGCATTGGAAAATCCAACACCAAGGACATCACAGAAGTTACTGCTGTGG CTGAAGCCATCCTCCCTAAGGGCAGTGCCCGAGTCACAACTGCGGTGAGGAAAGCCTTTCCTGCCT CCCAAACACGCTCCATAGGAATGCCTAGAAAAGGCAGTTCTTGTGTCCTTATGTTCTGTAAATCATTT GGGATAGTCTCTCGATTTAGGCTCTGAGAAGGTGTGTGCCAATTACTCACTCTTTGGCTGGTCTGTC TGTCTCTATAGGTGAAGTTTAGTGCTCCATCTTTGTTGTATGGTGCTCTCCGAGACTATCAGAAGATA GGCCTGGACTGGTTGGCCAAGCTATACCGGAAGAATCTCAATGGCATAT*TGGCTGATGAAGCAGGG* *CTT*GGC**GCC**ACTGTGCAGATCATTGCTTTTTTTGCTCACCTTGCCTGTAATGAAGGTAAGATCCTCTC AGTCTCCACTAAGAGCGTGTGTTAGATCTGAGAGAAAAGAAATTGTCAGCCTCTTTTGCTCATCTCTC TTTCTTGAGCCAAGAAATGACTCTCCTTTTTAAAATTTTTATTTATTTTTTTATTCTTTGCATACATTATA TCTCGACCACACCATTCTTCCCAGAGTCTTCCTCCATCATCTTCTCCCCAGGAGCTTCCATTACCATA AAAAAATAAAACCAACAAATAACAGCAACAAAAAACAAAAAGCAGGCATCCCAGGGATATCCACCATA CATGGCATAACAAGTTACAGTGAGACTAGGCACAAACCCTCATCTCAAGGCTGGATGAGGCAGCCC AGTAGA

Supplemental Methods

Deep sequencing data analysis

RNA-seq

TopHat2 (Kim et al., 2013) was used to map the RNAseq reads to the mouse genome (mm10) using parameters (--library-type fr-firststrand --segment-length 38). The bam files from the Tophat output were used for downstream analysis using HOMER (Heinz et al., 2010). DESeq2 (Love et al., 2014) was used to identify the differentially expressed genes. Heatmaps were generated using Java TreeView (Saldanha, 2004). K-means clustering was performed using Cluster 3.0 (de Hoon et al., 2004), and GO term enrichment was calculated using Metascape software (http://metascape.org) (Tripathi et al., 2015).

ATAC-seq

Paired-end 75 bp reads were trimmed to 24 bases and reads were then aligned to mm10 using Bowtie2 with the parameter -X 2000 to ensure that fragments up to 2 kb were allowed to align. Duplicates were then removed using Picard (http://broadinstitute.github.io/picard/). Reads with low quality score (MAPQ < 10) and reads mapping to the mitochondrial genome (chrM) were removed. Reads were separated into size classes as described (Buenrostro et al., 2013) and only nucleosome free reads (less than 100 bp) were used for subsequent analyses. These reads were processed in HOMER (Heinz et al., 2010). Genome browser tracks were generated from mapped reads using the "makeUCSCfile" command. Mapped reads were aligned over specific regions using the "annotatePeaks" command to make 20 bp bins over regions of interest and sum the reads within each bin. Experiments were aligned over high quality (peak score > 6) Tip60 peaks called from (Ravens et al., 2015), that were subsequently separated into

promoter-proximal and –distal groups. After anchoring mapped reads over reference sites, aggregation plots were generated by averaging data obtained from biological replicates. Heatmaps were ordered based on clustering of reads summed over -100 bp to +100 bp from the Tip60 peak center through K-means clustering using Cluster 3.0.

ChIP-seq

Single-end raw FastQ reads were collapsed, adaptor sequence were removed, and reads were mapped to the mouse mm10 genome using bowtie, allowing one mismatch. Aligned reads were used for downstream analysis using the "annotatePeaks" command in HOMER (Heinz et al., 2010) to make 20 bp bins over promoter proximal regions and summing the reads within each bin. Experiments were aligned over high quality (peak score > 6) promoter-proximal Tip60 peaks called from (Ravens et al., 2015). After anchoring mapped reads over the reference site, heatmaps for biological replicates were generated using Java Treeview.

Supplemental References

Buenrostro, J.D., Giresi, P.G., Zaba, L.C., Chang, H.Y., Greenleaf, W.J., 2013. Transposition of native chromatin for fast and sensitive epigenomic profiling of open chromatin, DNA-binding proteins and nucleosome position. Nat Meth 10, 1213–1218. doi:10.1038/nmeth.2688

de Hoon, M.J.L., Imoto, S., Nolan, J., Miyano, S., 2004. Open source clustering software. Bioinformatics 20, 1453–1454. doi:10.1093/bioinformatics/bth078

Heinz, S., Benner, C., Spann, N., Bertolino, E., Lin, Y.C., Laslo, P., Cheng, J.X., Murre, C., Singh, H., Glass, C.K., 2010. Simple combinations of lineage-determining transcription factors prime cis-regulatory elements required for macrophage and B cell identities. Mol Cell 38, 576–589. doi:10.1016/j.molcel.2010.05.004

Kim, D., Pertea, G., Trapnell, C., Pimentel, H., Kelley, R., Salzberg, S.L., 2013. TopHat2: accurate alignment of transcriptomes in the presence of insertions, deletions and gene fusions. Genome Biol. 14, R36. doi:10.1186/gb-2013-14-4-r36

Love, M.I., Huber, W., Anders, S., 2014. Moderated estimation of fold change and dispersion for RNA-seq data with DESeq2. Genome Biol. 15, 550. doi:10.1186/s13059-014-0550-8

Ravens, S., Yu, C., Ye, T., Stierle, M., Tora, L., 2015. Tip60 complex binds to active Pol II promoters and a subset of enhancers and co-regulates the c-Myc network in mouse embryonic stem cells. Epigenetics & Chromatin 8, 45. doi:10.1186/s13072-015-0039-z

Saldanha, A.J., 2004. Java Treeview--extensible visualization of microarray data. Bioinformatics 20, 3246–3248. doi:10.1093/bioinformatics/bth349

Tripathi, S., Pohl, M.O., Zhou, Y., Rodriguez-Frandsen, A., Wang, G., Stein, D.A., Moulton, H.M., DeJesus, P., Che, J., Mulder, L.C.F., Yángüez, E., Andenmatten, D., Pache, L., Manicassamy, B., Albrecht, R.A., Gonzalez, M.G., Nguyen, Q., Brass, A., Elledge, S., White, M., Shapira, S., Hacohen, N., Karlas, A., Meyer, T.F., Shales, M., Gatorano, A., Johnson, J.R., Jang, G., Johnson, T., Verschueren, E., Sanders, D., Krogan, N., Shaw, M., König, R., Stertz, S., García-Sastre, A., Chanda, S.K., 2015. Meta- and Orthogonal Integration of Influenza ``OMICs"" Data Defines a Role for UBR4 in Virus Budding. Cell Host and Microbe 18, 723–735. doi:10.1016/j.chom.2015.11.002